

Earthquake performance evaluation of three-dimensional roller compacted concrete dams

Murat Emre Kartal^{1a} and Muhammet Karabulut^{*2}

¹Department of Engineering Faculty, Izmir Democracy University, Izmir, Turkey

²Department of Civil Engineering, Bulent Ecevit University, Zonguldak, Turkey

(Received September 11, 2017, Revised February 8, 2018, Accepted February 10, 2018)

Abstract. A roller compacted concrete (RCC) dam should be analyzed under seismic ground motions for different conditions such as empty reservoir and full reservoir conditions. This study presents three-dimensional earthquake response and performance of a RCC dam considering materially non-linearity. For this purpose, Cine RCC dam constructed in Aydin, Turkey, is selected in applications. The three-dimensional finite element model of Cine RCC dam is obtained using ANSYS software. The Drucker-Prager material model is considered in the materially nonlinear time history analyses for concrete and foundation rock. Furthermore, hydrodynamic effect was investigated in linear and non-linear dynamic analyses. Researchers observe that how the tensile and compressive stresses change by hydrodynamic pressure effect. The hydrodynamic pressure of the reservoir water is modeled with the fluid finite elements based on the Lagrangian approach. In this study, dam body and foundation are modeled with welded contact. The displacements and principle stress components obtained from the linear and non-linear analyses with and without reservoir water are compared each other. Principle stresses during earthquake were obtained at the most critical point in the upstream face of dam body. Besides, the change of displacements and stresses by crest length were investigated. Moreover demand-capacity ratio criteria were also studied under linear dynamic and nonlinear analysis. Earthquake performance analyses were carried out for different cases and evaluated. According to linear and nonlinear analysis, hydrodynamic water effect is obvious in full reservoir situation. On the other hand, higher tensile stresses were observed in linear analyses and then non-linear analyses were performed and compared with each other.

Keywords: demand-capacity ratio; Lagrangian approach; non-linear dynamic analysis; performance analysis; roller compacted concrete dam

1. Introduction

Human being always needs water supply for drinking, cleaning, farming, livestock fattening, irrigation, electricity and other basic things from the earliest age until now. For this purpose, people have tried to settle around water supplies and they have preferred to live in those places. However, the human population increases quickly in the modern world and to a very high level and therefore people need to construct water storages day by day. Then human started to build huge water storages and dams. Civil engineers have enhanced the dams with new constructing techniques by technological measuring devices, experiments and modern computer software. We can see lots of dam types and they continue to increase in quantity all over the world. In this study, we select a roller compacted concrete (RCC) dam for investigation of seismic response and performance analysis.

A roller compacted concrete (RCC) dam is designed as traditional concrete structures. But concrete design and

construction techniques are different in RCC dams. These techniques have some advantages such as rapid placement and economically benefits for construction. RCC dams drier than other dam types. Vibratory rollers, dozers and other heavy equipment are used in RCC dams' constructions. Construction procedures associated with RCC require particular attention were given in the layout and design to water tightness and seepage control, horizontal and transverse joints, facing elements, and appurtenant structures (Kartal 2012). In the hardened condition, mechanical properties of RCC dams take after those of conventional concrete dams (USACE 1995). Engineers do not want any leakage problem from upstream face to downstream side. So, the researchers have analyzed thermal cracking problems due to these cracks may lead undesirable situations. Noorzai *et al.* (2006) investigated Kinta RCC gravity dam thermal and structural aspects. Kinta RCC gravity dam was modeled two dimensional, which is the first dam in Malaysia, by finite element code. After all analyses, they observed results of Kinta dam between obtaining finite element code results and actually temperatures measured results. The Shapai roller-compacted concrete (RCC) arch dam and the Zipingpu concrete-faced rockfill (CFR) dam were analyzed the hazards and seismic performance of reservoirs and typical large dams based on a field investigation following the Wenchuan (MW=8.0) earthquake (Lin *et al.* 2014). Wang *et*

*Corresponding author, Ph.D. Student

E-mail: karabulut@beun.edu.tr

^aPh.D.

E-mail: murat.kartal@idu.edu.tr

al. (2015) investigated the seismic performance of concrete gravity dams, both the linear and nonlinear analysis methods considering the dam-reservoir-foundation interaction are adopted in their study. They used demand capacity ratio, cumulative overstress duration and spatial extent of overstressed for determined the stress and cracks in the study. According to linear dynamic analyses, a two-component ground motion with longer integrated duration tends to cause larger overstressed region and longer cumulative overstress duration. Besides, the nonlinear damage-plastic analysis shows that a two-component ground motion with longer integrated duration might lead to greater and also more dangerous cracks. Furthermore, Monteiro and Barros (2008) are considered horizontal and vertical accelerations of the seismic action in their study. Zhang and Wang (2013) focused on nonlinear dynamic response of a concrete gravity dam considering near-field and far-fault ground motion influences. Ghaedi *et al.* (2015) studied the seismic analysis of roller compacted concrete (RCC) dams. Yazdani and Alembagheri (2017) evaluated nonlinear seismic response of a gravity dam considering near-fault ground motion. They used full reservoir condition in nonlinear time-history analyses. Liu *et al.* (2015) studied on real-time construction quality monitoring of storehouse surfaces for RCC dams. They investigated that construction quality is in roller compacted concrete (RCC) dams. Alembagheri and Ghaemian (2013) presented the damage assessment of a concrete arch dam. They used nonlinear incremental dynamic analysis in their study. The dam-foundation interaction effects have been investigated by varying foundation's and concrete's modulus of elasticities. Yilmazturk *et al.* (2015) evaluated seismic assessment of a monolithic RCC gravity dam. They considered three-dimensional dam-foundation-reservoir interaction in this study. According to the study, the importance and necessity of a full 3D analyses for such systems were underlined by comparing the results with two dimensional analyses. Zhang *et al.* (2009) presented relocating mesh method for the computation of temperature field of RCC dam. They focus on feasibility and error of the relocating mesh method. According to results, the method has high calculation precision, less computer run time and less memory.

Strong ground motion can affect huge water structures and can damage seriously. The primary aim of this research is that reveal a RCC dam behavior during a strong ground motion effect and evaluate its performance of for a selected dam. In this study, Cine RCC dam was modeled by finite element method with ANSYS software. The material properties were obtained from the experimental data of the dam. Three-dimensional finite element dam model was considered for empty and full reservoir conditions. We evaluated the dam for four different cases. The dam model has fixed boundary condition for all cases. Each case results compared with each other. Comparing all case results give an information about hydrodynamic water effect on dam, we can observe serious differences between principle stress results according to linear and non-linear time history analysis in these cases.

All dynamic analyses were performed under 1989 Loma Prieta earthquake records. The horizontal displacements,

principle tensile and compressive stresses for empty and full reservoir conditions were compared with each other. Besides, the most critical point in dam body was investigated by performance analysis for linear and nonlinear analysis. After the performance analysis, Demand/Capacity (D/C) and principle stresses graphics have obtained for four cases at the most critical location in the upstream side of the dam. Furthermore, using the D/C-principle stresses graphics we were able to determine the cumulative inelastic duration and demand-capacity (D/C) ratio graphs. We can consider the safety and damaging of Cine dam if it shakes under this kind of strong ground motion using demand capacity ratio graphs. Because the graphics relevant with the allowable stresses limits and they show us over these lines or not.

2. Formulation of dam-foundation-reservoir interaction by the Lagrangian approach

Wilson and Khalvati (1983) used the formulation of the fluid system based on the Lagrangian approach is presented as following. In this approach, fluid is assumed to be linearly compressible, inviscid and irrotational. For a general three-dimensional fluid, pressure-volumetric strain relationships can be written in matrix form as follows

$$\begin{Bmatrix} P \\ P_x \\ P_y \\ P_z \end{Bmatrix} = \begin{bmatrix} C_{11} & 0 & 0 & 0 \\ 0 & C_{22} & 0 & 0 \\ 0 & 0 & C_{33} & 0 \\ 0 & 0 & 0 & C_{44} \end{bmatrix} \begin{Bmatrix} \varepsilon_v \\ w_x \\ w_y \\ w_z \end{Bmatrix} \quad (1)$$

where P , C_{11} , and ε_v are the pressures which are equal to mean stresses, the bulk modulus and the volumetric strains of the fluid, respectively. Since irrationality of the fluid is considered (Bathe 1996) like penalty methods, rotations and constraint parameters are included in the pressure-volumetric strain equation (Eq. (1)) of the fluid. In this equation P_x , P_y , P_z , is the rotational stress; C_{22} , C_{33} , C_{44} are the is the constraint parameters and w_x , w_y and w_z are the rotations about the Cartesian axes x , y and z .

In this study, the equations of motion of the fluid system are obtained using energy principles. Using the finite element approximation, the total strain energy of the fluid system may be written as

$$\pi_e = \frac{1}{2} \mathbf{U}_f^T \mathbf{K}_f \mathbf{U}_f \quad (2)$$

where \mathbf{U}_f and \mathbf{K}_f are the nodal displacement vector and the stiffness matrix of the fluid system, respectively. \mathbf{K}_f is obtained by the sum of the stiffness matrices of the fluid elements as follows

$$\begin{aligned} \mathbf{K}_f &= \sum \mathbf{K}_f^e \\ \mathbf{K}_f^e &= \int_v \mathbf{B}_f^e{}^T \mathbf{C}_f \mathbf{B}_f^e dV^e \end{aligned} \quad (3)$$

where \mathbf{C}_f is the elasticity matrix consisting of diagonal terms in Eq. (1). \mathbf{B}_f^e is the strain-displacement matrix of the fluid element.

An important behavior of fluid systems is the ability to displace without a change in volume. For reservoir and storage tanks, this movement is known as sloshing waves in which the displacement is in the vertical direction. The increase in the potential energy of the system because of the free surface motion can be written as

$$\pi_s = \frac{1}{2} \mathbf{U}_{sf}^T \mathbf{S}_f \mathbf{U}_{sf} \quad (4)$$

where U_{sf} and S_f are the vertical nodal displacement vector and the stiffness matrix of the free surface of the fluid system, respectively. S_f is obtained by the sum of the stiffness matrices of the free surface fluid elements as follows

$$\left. \begin{aligned} \mathbf{S}_f &= \sum \mathbf{S}_f^e \\ \mathbf{S}_f^e &= \rho_f g \int_{\mathbf{A}} \mathbf{h}_s^T \mathbf{h}_s dA^e \end{aligned} \right\} \quad (5)$$

where h_s is the vector consisting of interpolation functions of the free surface fluid element. ρ_f and g are the mass density of the fluid and the acceleration due to gravity, respectively. Besides, kinetic energy of the system can be written as

$$\mathbf{T} = \frac{1}{2} \dot{\mathbf{U}}_f^T \mathbf{M}_f \dot{\mathbf{U}}_f \quad (6)$$

where \dot{U}_f and M_f are the nodal velocity vector and the mass matrix of the fluid system, respectively. M_f is also obtained by the sum of the mass matrices of the fluid elements as follows

$$\left. \begin{aligned} \mathbf{M}_f &= \sum \mathbf{M}_f^e \\ \mathbf{M}_f^e &= \rho_f \int_{\mathbf{V}} \mathbf{H}^T \mathbf{H} dV^e \end{aligned} \right\} \quad (7)$$

where H is the matrix consisting of interpolation functions of the fluid element. if (Eq. (2), (4) and (6)) are combined using the Lagrange's equation (Clough and Penzien 1993); the following set of equations is obtained

$$\mathbf{M}_f \ddot{\mathbf{U}}_f + \mathbf{K}_f^* \mathbf{U}_f = \mathbf{R}_f \quad (8)$$

where K_f^* , \ddot{U}_f , U_f and R_f are the system stiffness matrix including the free surface stiffness, the nodal acceleration and displacement vectors and time-varying nodal force vector for the fluid system, respectively. In the formation of the fluid element matrices, reduced integration orders (Wilson and Khalvati 1983).

The equations of motion of the fluid system, (Eq. (8)), have a similar form with those of the structure system. To obtain the coupled equations of the fluid-structure system, the determination of the interface condition is required. Since the fluid is assumed to be inviscid, only the displacement in the normal direction to the interface is continuous at the interface of the system. Akkas *et al.* (1979) assumed that the structure has the positive face and the fluid has the negative face, the boundary condition at the fluid-structure interface is

$$\mathbf{U}_n^- = \mathbf{U}_n^+ \quad (9)$$

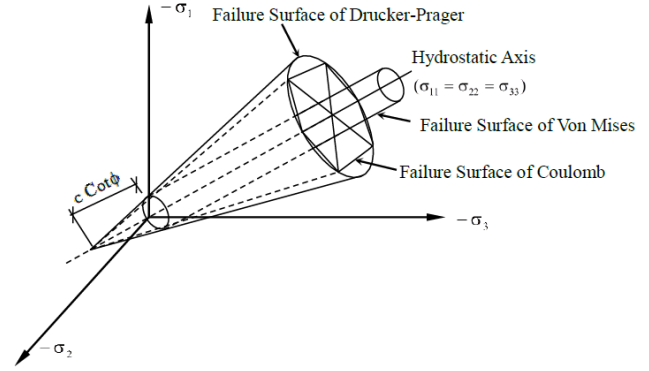


Fig. 1 Failure criteria for Coulomb, Drucker-Prager and von Mises used by Chen and Mizuno (1990)

where U_n is the normal component of the interface displacement. Using the interface condition, the equation of motion of the coupled system to ground motion including damping effects are given by

$$\mathbf{M}_c \ddot{\mathbf{U}}_c + \mathbf{C}_c \dot{\mathbf{U}}_c + \mathbf{K}_c \mathbf{U}_c = \mathbf{R}_c \quad (10)$$

in which M_c , C_c , and K_c are the mass, damping and stiffness matrices for the coupled system, respectively. U_c , \dot{U}_c , \ddot{U}_c and R_c are the vectors of the displacements, velocities, accelerations and external loads of the coupled system, respectively.

3. The Drucker-Prager model

There are many criteria for determination of yield surface or yield function of materials. The Drucker-Prager criterion is widely used for frictional materials such as rock and concrete. Drucker and Prager (1952) obtained a convenient yield function to determine elasto-plastic behavior of concrete smoothing Mohr-Coulomb criterion (Fig. 1). This function is defined (Chen and Mizuno 1990) as

$$f = \alpha I_1 + \sqrt{J_2} - k \quad (11)$$

where α and k are constants which depend on cohesion (c) and angle of internal friction (ϕ) of the material given by

$$\left. \begin{aligned} \alpha &= \frac{2 \sin \phi}{\sqrt{3} (3 - \sin \phi)} \\ k &= \frac{6c \cos \phi}{\sqrt{3} (3 - \sin \phi)} \end{aligned} \right\} \quad (12)$$

In Eq. (11), I_1 is the first invariant of stress tensor (σ_{ij}) formulated as follows

$$I_1 = \sigma_{11} + \sigma_{22} + \sigma_{33} \quad (13)$$

and J_2 is the second invariant of deviatoric stress tensor (s_{ij}) given by

$$J_2 = \frac{1}{2} s_{ij} s_{ij} \quad (14)$$

where, s_{ij} is the deviatoric stresses as yielded below.

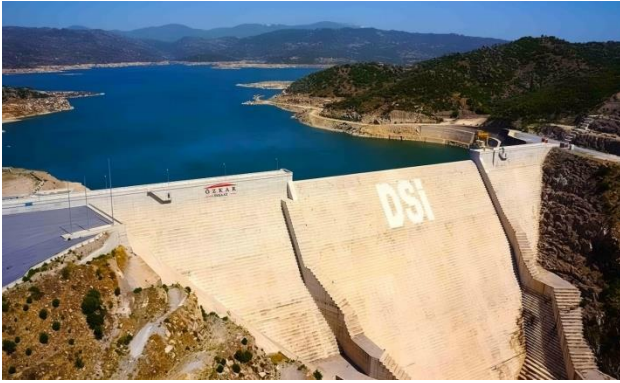


Fig. 2 The general view of Cine RCC dam

$$s_{ij} = \sigma_{ij} - \delta_{ij} \sigma_m \quad (i, j=1,2,3) \quad (15)$$

In Eq. (15), δ_{ij} is the Kronecker delta, which is equal to 1 for $i=j$; 0 for $i \neq j$, and σ_m is the mean stress and obtained as follows

$$\sigma_m = \frac{I_1}{3} = \frac{\sigma_{ii}}{3} \quad (16)$$

If the terms in Eq. (15) are obtained by Eq. (16) and replaced in Eq. (14), the second invariant of the deviatoric stress tensor can be obtained as follows

$$J_2 = \frac{1}{6} \left[(\sigma_{11} - \sigma_{22})^2 + (\sigma_{22} - \sigma_{33})^2 + (\sigma_{33} - \sigma_{11})^2 \right] + \sigma_{12}^2 + \sigma_{13}^2 + \sigma_{23}^2 \quad (17)$$

4. Mathematical model of Cine RCC dam

4.1 Cine dam

Cine dam, located approximately 16 km southeast of Cine, Aydın, was constructed in 2010 by General Directorate of State Hydraulic Works (Fig. 2). It was established on Cine River. This dam was projected as a roller compacted concrete dam. Its reservoir is used for irrigation and energy purposes. The dam crest is 372.5 m in length and 9 m in wide. The maximum height and base width of the dam are 136.5 m and 142.5 m, respectively. The maximum height of the reservoir water is considered as 98.77 m. The annual total power generation capacity is 118 GW.

4.2 Material properties of Cine RCC dam

The three-dimensional finite element model of Cine dam is modelled considering two layered foundation with gneiss rock. Material properties of Cine roller compacted concrete dam body and foundation are given in Table 1. The cohesion for the parent RCC have ranged from as little as 0.5 MPa and less to over 4.1 MPa (Luhr 2000).

4.3 Finite element model of Cine dam

This study considers three-dimensional finite element

Table 1 Material properties of Cine dam

	Material Properties					
	Modulus of elasticity (MPa)	Poisson's ratio	Mass density (kg/m ³)	Cohesion (kPa)	Angel of internal friction	Angel of dilatation
Concrete (Dam Body)	2.50E4	0.2	2500	900	41	11
Blocky gneiss (foundation)	1.75E4	0.15	2400	4000	39	9
Very blocky gneiss (valley)	1.4E4	0.15	2400	3000	38	8

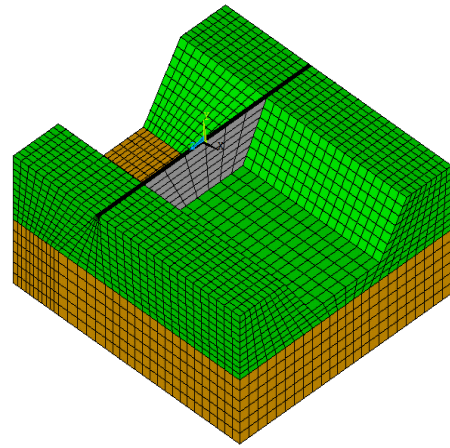


Fig. 3 Finite element model of Cine dam for empty reservoir condition

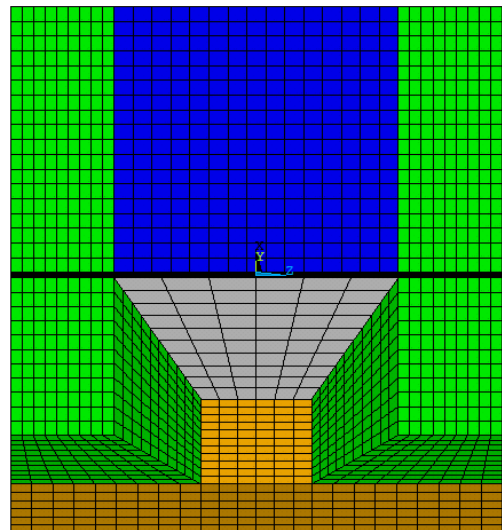


Fig. 4 Finite element model of Cine dam for full reservoir condition

model (FEM) of Cine RCC dam with fixed boundary conditions (Figs. 3 and 4). In this model, if the height of the dam is indicated as ' H ', the foundation soil is extended as ' H ' in the downstream river direction and gravity direction. Besides, foundation soil and reservoir water model is extended as ' $3H$ ' in the upstream direction. Fluid and solid

Table 2 Case properties

Case Numbers	Reservoir	Boundary	Connection	Analysis Type
Case 1	Empty	Fixed	Welded	Linear
Case 2				Non-linear
Case 3	Full			Linear
Case 4				Non-linear

element matrices are computed using the Gauss numerical integration technique. SOLID 45 elements were used to modelling dam body, foundation and valley part of Cine dam. Besides, reservoir water modelled by Lagrangian Approach using FLUID 80 elements.

In this study, we modelled the RCC dam with and without water to observe the effect of hydrodynamic on the earthquake behavior of the dam. The three-dimensional finite element model of Cine RCC dam is obtained using finite element method by ANSYS software. We determined maximum principle tensile and compressive stresses for the bottom point of upstream side of dam body.

4.4 Numerical analysis cases

We investigated 4 different cases in the scope of this study. We present different analysis cases for reservoir conditions in Table 2. The aim of these cases is to reveal the effect of the hydrodynamic pressure and non-linear response of the dam separately.

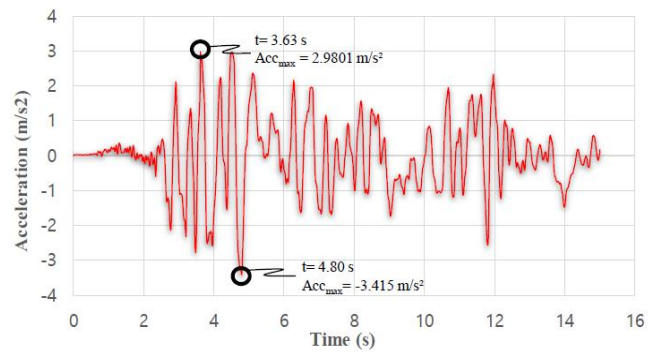
4.5 Loma Prieta 1989 earthquake records

An earthquake severely shaken San Francisco and Monterey Bay regions at 5:04:15 p.m. on October 17, 1989. Epicenter point is 37.04° north latitude and 121.88° west longitude near Loma Prieta peak in the Santa Cruz Mountains. The depth of the earthquake is 18 km and extended 35 km along the fault. John *et al.* (1999) determined the earthquake moment magnitude is 7.1 Md.

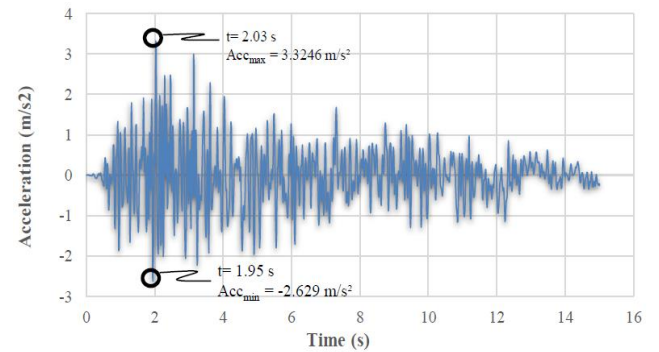
In this study, east-west, north-south and vertical components of earthquake were used. The accelerograms of the earthquake are given in Fig. 5. The earthquake duration time is 15 seconds and sampling interval is 0.01 second in the earthquake analyses.

5. Numerical analysis and results

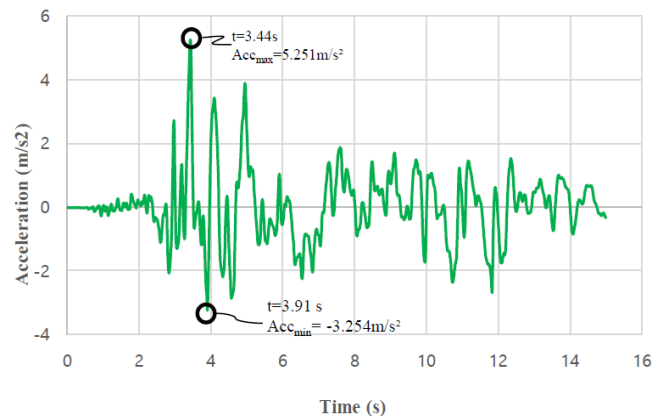
We investigated Cine RCC dam by three aspects for the 4 different cases stated in the previous section. First of these aspects is maximum-minimum displacements and principle tensile stress components during earthquake throughout crest length. The second one is the displacements and stress components changing by dam body height. The third one is the principle tensile and compressive stresses changing by time at the most critical point. Graphics and contour diagrams of the linear and nonlinear analyses in empty reservoir condition (Case 1-2) and full reservoir condition (Case 3-4) according to numerical analyses were given as follows.



(a) East-West direction



(b) North-South direction



(c) Vertical direction

Fig. 5 The Loma Prieta 1989 Earthquake records

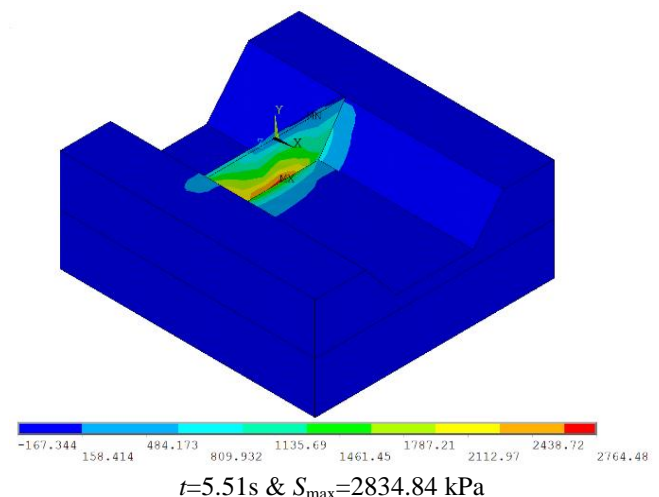


Fig. 6 The maximum principle tensile stress in Case 1

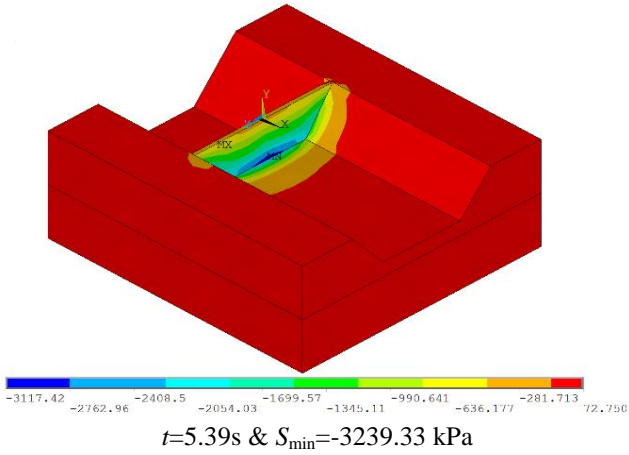


Fig. 7 The minimum principle compressive stress in Case 1

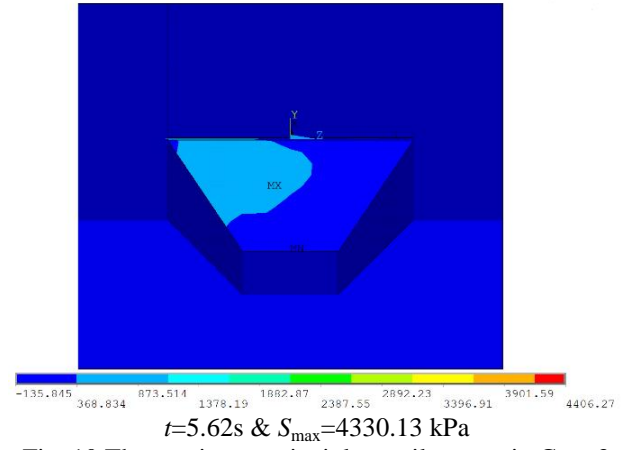


Fig. 10 The maximum principle tensile stress in Case 3

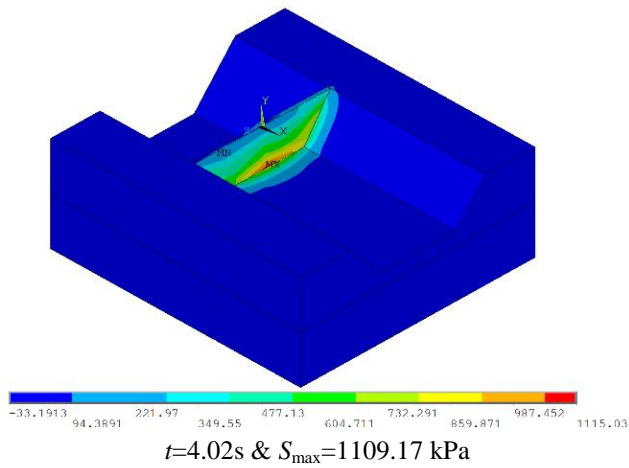


Fig. 8 The maximum principle tensile stress in Case 2

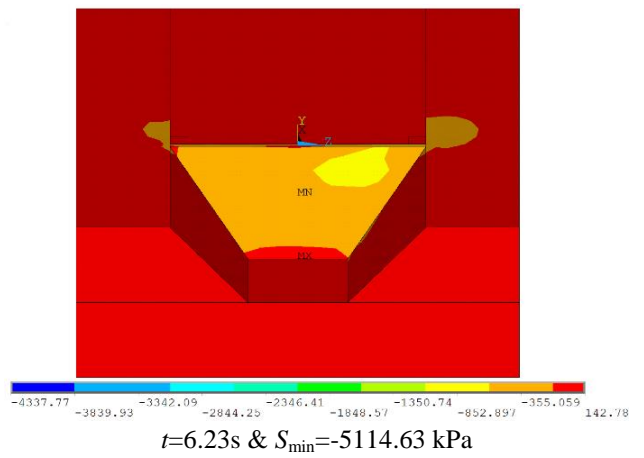


Fig. 11 The minimum principle compressive stress in Case 3

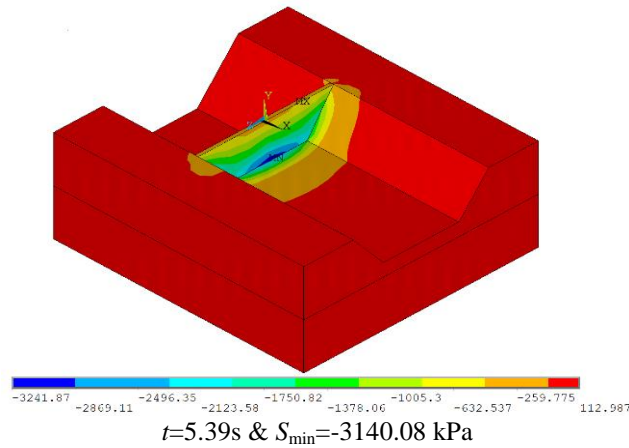


Fig. 9 The minimum principle compressive stress in Case 2

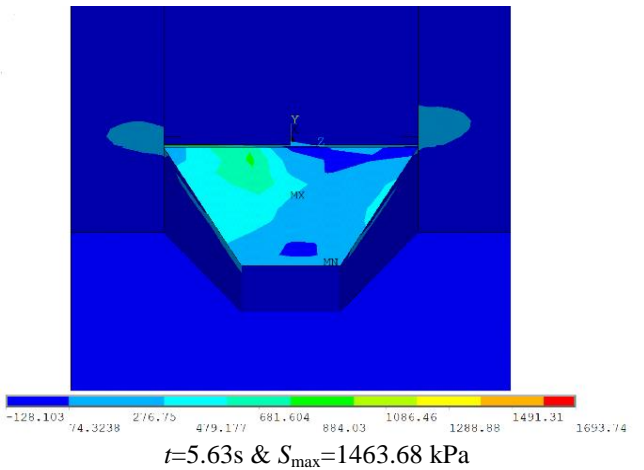


Fig. 12 The maximum principle tensile stress in Case 4

According to linear and nonlinear dynamic analyses, we investigated earthquake response of the Cine dam with various different aspects. Firstly, maximum and minimum horizontal displacements changing throughout the crest were given in Fig. 14. We can clearly observe the hydrodynamic effect of the reservoir water on crest with the increased horizontal displacement.

Secondly, tensile stresses were obtained at the selected point in all cases. The tensile stresses during earthquake were compared in both linear and nonlinear analyses for empty and full reservoir conditions in Fig. 15. Maximum tensile stresses are given in the same order 2834.84 kPa, 1109.17 kPa, 4330.13 kPa and 1463.68 kPa in Case 1, Case 2, Case 3 and Case 4. It is seemed that linear analysis results are higher than nonlinear analysis results as

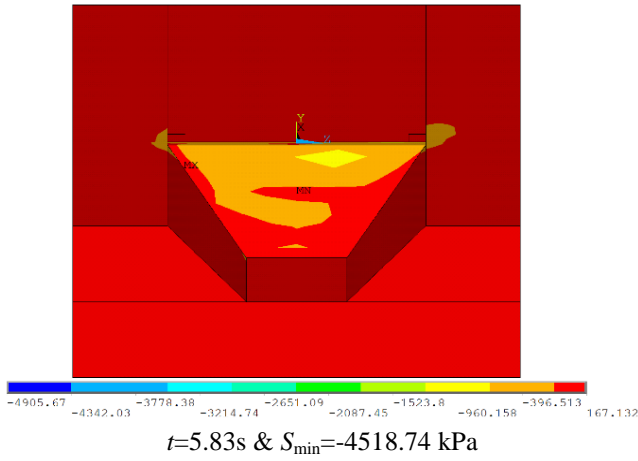
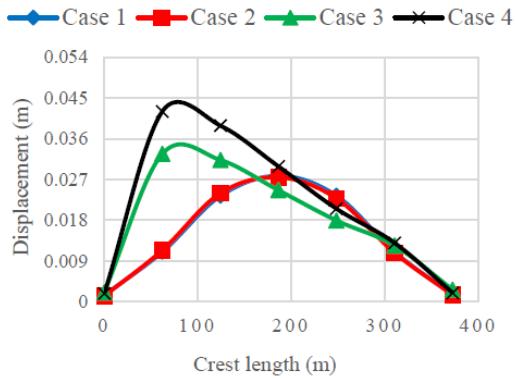
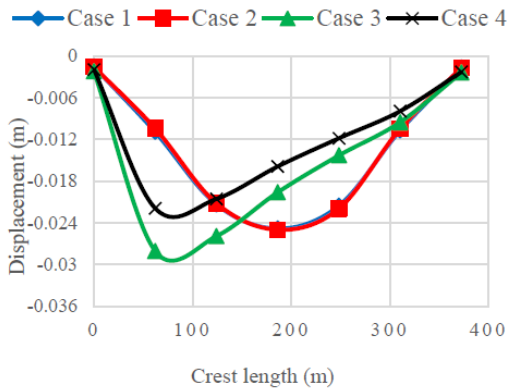


Fig. 13 The minimum principle compressive stress in Case 4



(a) Maximum displacements on crest

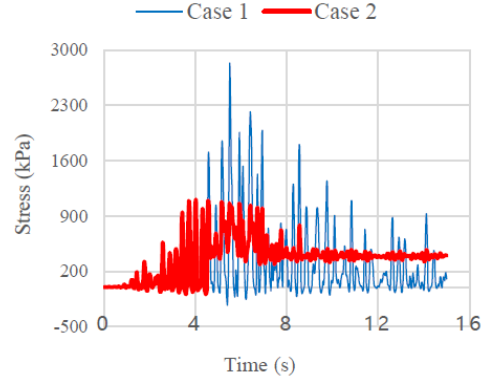


(b) Minimum displacements on crest

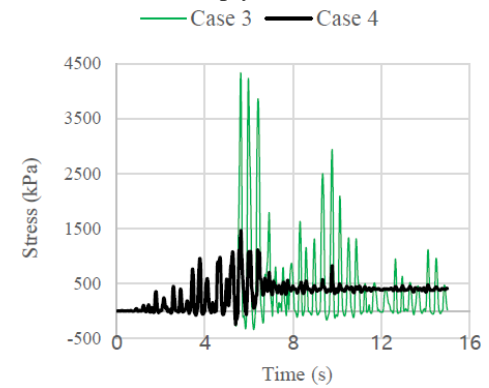
Fig. 14 Maximum and minimum horizontal displacements throughout the crest

expected. Besides, full reservoir cases have higher tensile stresses than empty reservoir cases.

Thirdly, compressive stresses were gathered from four cases. Maximum compressive stresses are given as -3239.33 kPa, -3140.08 kPa, -5114.63 kPa and -4518.74 kPa in Case 1-2-3-4 respectively. The results were categorized full-empty and nonlinear-linear the values have been given in Fig. 16. Linear analysis results in full reservoir condition (Case 3) have the highest compressive stresses on the selected point. Besides, the nonlinear analysis results in

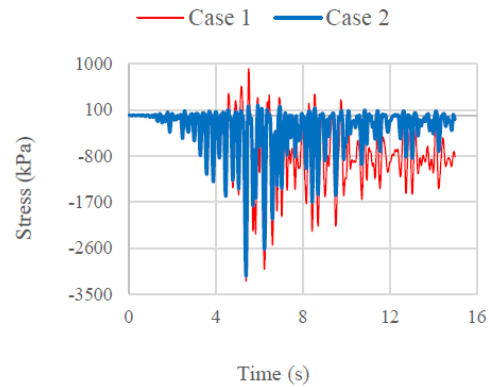


(a) Empty reservoir

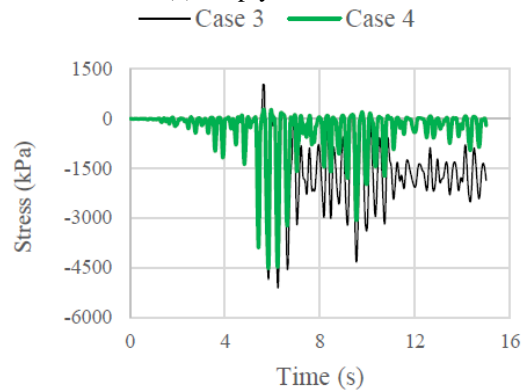


(b) Full reservoir

Fig. 15 Tensile stresses in linear and nonlinear analysis during earthquake

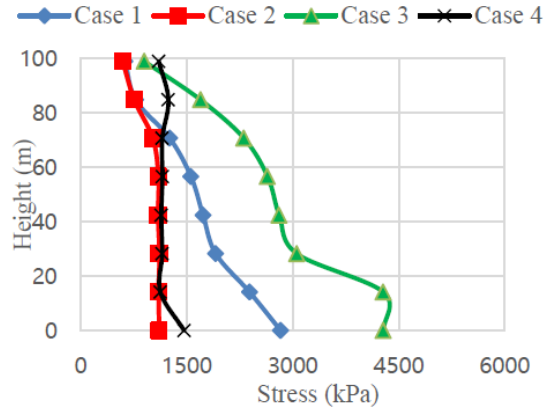


(a) Empty reservoir

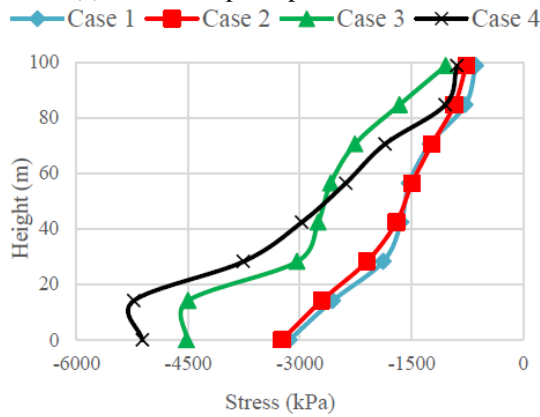


(b) Full reservoir

Fig. 16 Compressive stresses in linear and nonlinear analysis during earthquake



(a) Maximum principle tensile stresses



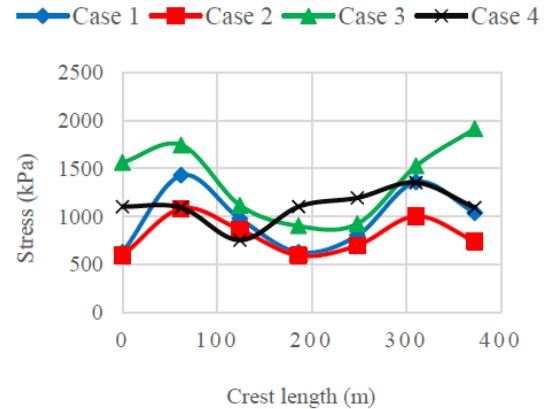
(b) Minimum principle compressive stresses

Fig. 17 The maximum and minimum principle stress components in the upstream face

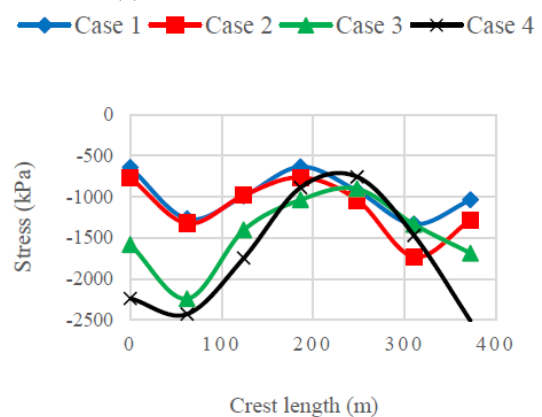
empty reservoir condition has smaller compressive stresses. Fourthly, maximum and minimum stresses changing by dam body height are given in Fig. 17. The higher tensile stresses occurred in Case 3 as expected. Other important point is that maximum and minimum stresses decrease from bottom to crest level. Empty reservoir and nonlinear analyses case, which is Case 2, has smaller tensile stresses throughout the dam than the other cases. Fifthly, top level of dam body which means on the crest region is examined stress aspect and maximum and minimum stresses have been calculated throughout the crest length. Maximum and minimum stresses changing by crest length have been given in Fig. 18. Finally, the maximum horizontal displacement is 3.1 cm on top point of dam body which is acceptable level for a RCC dam. Maximum and minimum horizontal displacements changing by dam height have been given Fig. 19.

6. Results of performance analysis

This section of the study describes a systematic approach for evaluation of the seismic performance and potential of damage using linear and nonlinear time-history analyses. Magnitudes of stress changing by time and cumulative inelastic duration of stresses were considered to explain the potential damage level. The level of probable



(a) Maximum stresses on crest



(b) Minimum stresses on crest

Fig. 18 The maximum and minimum principle stress components throughout the crest

damage is considered acceptable if the results from the linear elastic time history analyses fall below a specified threshold expressed in terms of cumulative inelastic duration and demand-capacity ratios. Otherwise the damage is considered severe requiring nonlinear methods of analyses (Ghannaat 2002). According to linear dynamic analyses, it was observed that lots of time the tensile stress of concrete over the threshold and nonlinear dynamic analyses of Cine RCC dam is necessary under earthquake records. All cases were investigated for probable damage by nonlinear analyses.

6.1 Demand-capacity ratios (DCR)

The demand-capacity ratio (DCR) for gravity and RCC dams is defined as the ratio of the calculated principal stress to tensile strength of the concrete. The tensile strength of the plain concrete used in calculation of DCR is gathered from the uni-axial splitting tension tests or from

$$ft = 1.7f'c^{\frac{2}{3}} \quad (18)$$

proposed by Raphael (1984), where $f'c$ is the compressive strength of the concrete.

6.2 Cumulative inelastic duration

Cumulative inelastic duration may be gathered roughly

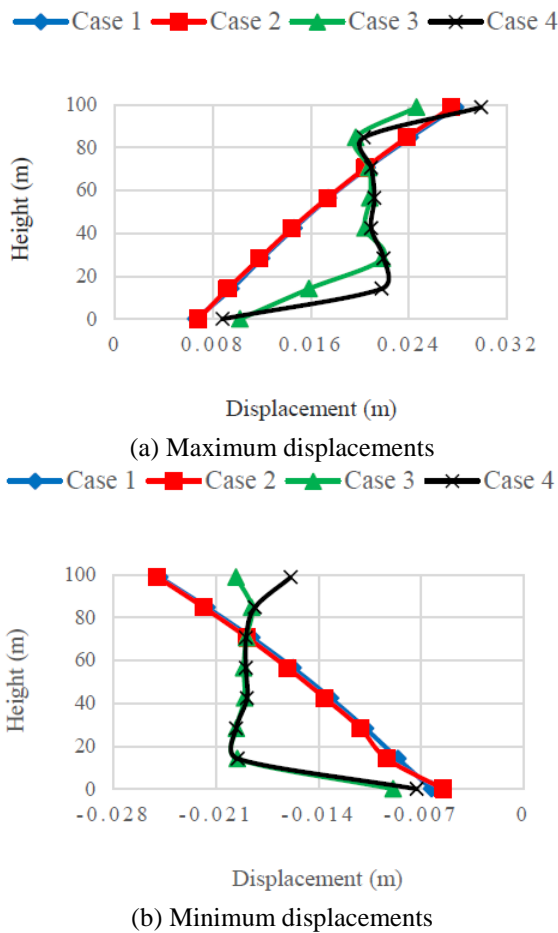


Fig. 19 Maximum and minimum horizontal displacements by dam height

by multiplying number of stress points over an accurate stress range by numeric time history analysis. The higher cumulative duration, the higher the possibilities for more damage. For RCC dams a lower cumulative duration of 0.3 is assumed, mainly because RCC dams resist loads by cantilever mechanism only, as opposed to arch dams that rely on both the arch and cantilever actions (U.S. Army Corps of Engineers 2016).

6.3 Performance criteria for RCC dams

The earthquake performance of RCC dams is evaluated on the basis of load combination cases, demand capacity ratios, and the related cumulative duration. The performance is formulated for the maximum design earthquake (MDE). The MDE is identified as the maximum range of earthquake for which a structure is designed (U.S. Army Corps of Engineers 2016). Three performance levels are considered:

Small or not damaging: Response of dam is considered to be within the linear elastic range of behavior with little or no possibility of damage if the calculated demand-capacity ratios are less than or equal to 1 ($D/C=1$).

Acceptable damage level: The dam will exhibit nonlinear response in the form of cracking and joint opening if the computed demand-capacity ratios exceed 1.0.

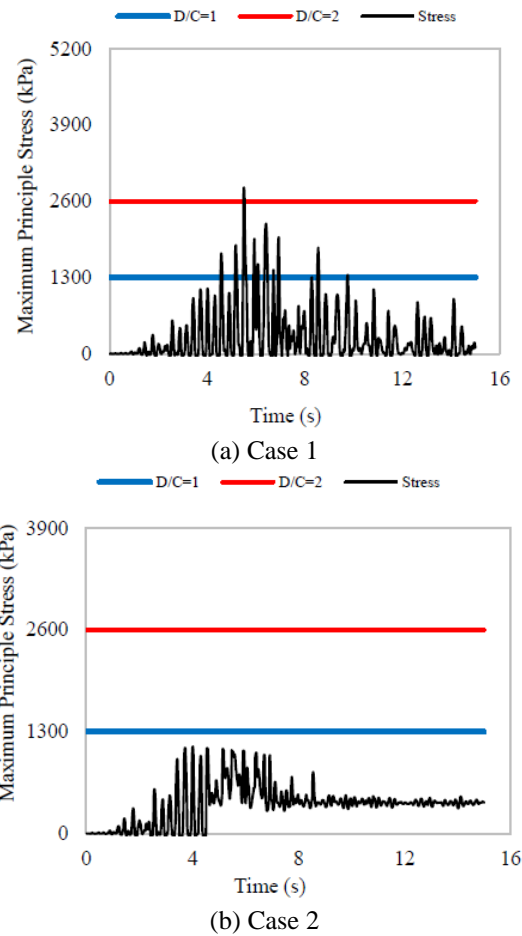
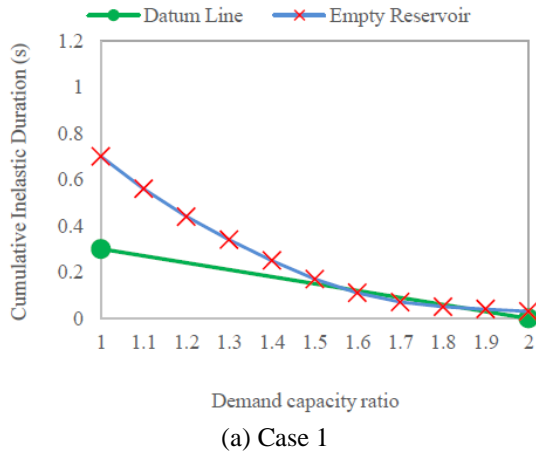


Fig. 20 The principle tensile stresses in empty reservoir condition during earthquake

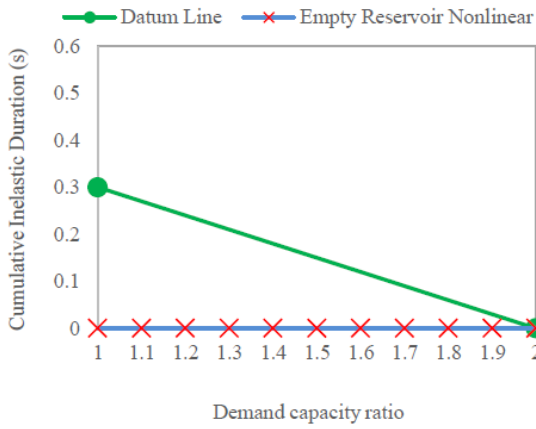
The level of nonlinear response or cracking is considered acceptable if stress demand-capacity ratios are less than 2.0 ($D/C=2$).

Severe damage: The damage is considered severe when demand-capacity ratios are greater than 2.0 ($D/C=2$). In these situations, a nonlinear time-history analysis may be required to assess the damage and thus the performance more accurately.

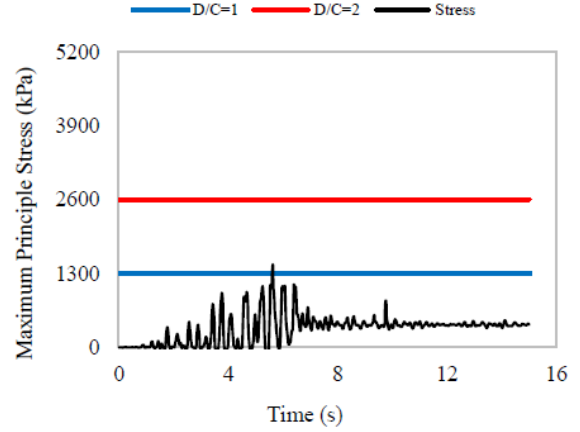
According to numeric time history analyses, principle stress-time graphs are drawn and they show how many times the stress value exceed the threshold in Figs. 20 and 22. Demand capacity ratio - cumulative inelastic duration graphs consist of principle stress and time components. We must examine the demand capacity ratio graphics in Figs. 21 and 23 for making a realistic comment on Cine RCC dam. When we check the Figs. 21(a), stresses are too high if compared the acceptable limit (datum line) in linear analyses. It shows that nonlinear analyses necessary to obtain more realistic results. After that, nonlinear time history analyses are completed and the results of them are given in Fig. 21(b). There are huge differences between linear and nonlinear demand capacity ratios in Fig. 21. We can observe clearly in Fig. 21(b), there is no stress value over the threshold in nonlinear analysis for empty reservoir condition and it displays smaller stresses than linear analysis.



(a) Case 1

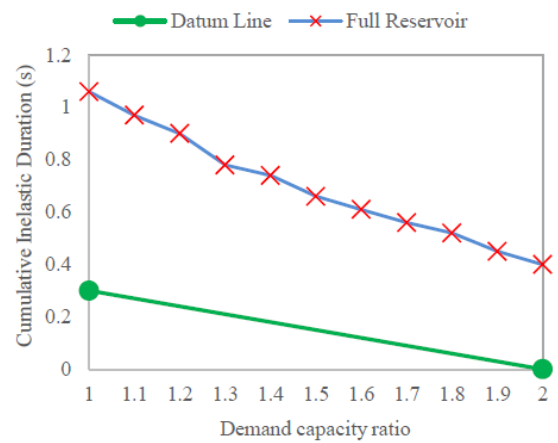


(b) Case 2

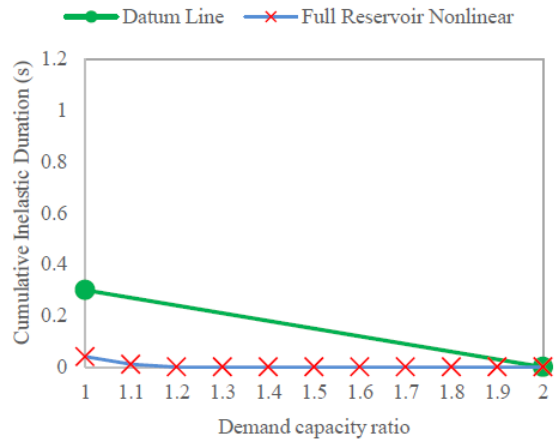


(b) Case 4

Fig. 22 Continued

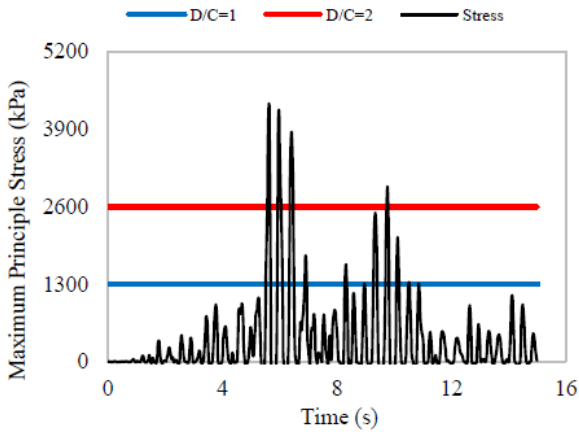


(a) Case 3



(b) Case 4

Fig. 21 The demand-capacity ratios in empty reservoir condition



(a) Case 3

Fig. 22 The principle tensile stresses in full reservoir condition during earthquake

Fig. 23 The demand-capacity ratios in full reservoir condition

In addition, the more important and deductive cases are Case 3 and 4 due to their full reservoir properties. Full reservoir condition and evaluation of its hydrodynamic effect on dam should carefully be examined. Because of that, we analyzed linearly and nonlinearly for full reservoir condition as well. According to linear analysis, it can be easily seen that reservoir effect is considerably obvious on principle stresses in Fig. 22(a) when we compare the Figs.

20(a) and Fig. 22(a). Besides, the most important case is Case 4 in this study due to the fact that it includes full reservoir and nonlinear analysis. Results of Case 4 have much more importance for dam safety criteria. Principle stresses gathered from Case 4 are given Fig. 23(b). When we compare Fig. 23(a) and (b), nonlinearity appears with reduced stresses in Figs. 23(b).

7. Conclusions

In this study, we performed three-dimensional finite element analyses of Cine RCC dam. Besides, we considered reservoir water by Lagrangian Approach. The Drucker-Prager material model was used in nonlinear time history analyses with fixed boundary condition. Loma Prieta 1989 earthquake records used in numerical dynamic analyses. The earthquake response of Cine RCC dam and evaluation of seismic performance have been presented. First of all, we examined dam behavior under strong ground motion effect. For this purpose, we carried out linear and nonlinear time-history analyses by ANSYS software considering empty and full reservoir conditions. The tensile-compressive stresses and horizontal displacements are compared in all cases. Then, we performed performance analysis of Cine RCC dam. Therefore, we selected the most critical points of the dam in the linear and non-linear performance analyses.

The tensile stresses obtained from linear analysis are higher than those in nonlinear analyses for empty reservoir condition.

The tensile stresses increase by the effect of the hydrodynamic pressure effect of the reservoir water in linear and non-linear analyses.

Nonlinear analyses give low and safer stresses in the numerical analyses.

While the hydrodynamic pressure of the reservoir decreases the earthquake performance of the dam and nonlinear response increases the earthquake performance.

Earthquake performance of the dam are under the acceptable level and it can be said that small or no damage appear in the dam in nonlinear analysis.

All analyses may be renewed for viscous or non-reflecting boundary conditions. It may result safer results for the response and performance of the dam.

References

- Akkas, N., Akay, H.U. and Yilmaz, Ç. (1979), "Applicability of general-purpose finite element programs in solid-fluid interaction problems", *Comput. Struct.*, **10**, 773-783.
- Alembagheri, M. and Ghaemian, M. (2013), "Damage assessment of a concrete arch dam through nonlinear incremental dynamic analysis", *Soil Dyn. Earthq. Eng.*, **44**, 127-137.
- Bathe, K.J. (1996), *Finite Element Procedures*.
- Chen, W.F. and Mizuno, E. (1990), *Nonlinear Analysis in Soil Mechanics - Theory and Implementation*.
- Clough, R. and Penzien, J. (1993), *Dynamics of Structures*.
- Drucker, C. and Prager, W. (1952), "Soil mechanics and plastic analysis of limit design", *Q. Appl. Math.*, **10**, 157-165.
- Ghaedi, K., Jameel, M., Ibrahim, Z. and Khanzaei, P. (2015), "Seismic analysis of roller compacted concrete (RCC) dams considering effect of sizes and shapes of galleries", *KSCE J. Civil Eng.*, **20**, 261-272.
- Ghanaat, Y. (2002), "Seismic performance and damage criteria for concrete dams", *Third US-Japan Work. Adv. Res. Earthq. Eng. Dams.*, 1-15.
- Nakata, J.K., Meyer, C.E., Wilshire, H.G., Tinsley, J.C., Updegrave, W.S., Peterson, D.M., ... and Diggles, M.F. (1999), "U.S. Geological survey", Charles G. Groat, Director, <https://pubs.usgs.gov/dds/dds-29/>.
- Kartal, M.E. (2012), "Three-dimensional earthquake analysis of

- roller-compacted concrete dams", *Nat. Hazard. Earthq. Syst.*, **12**, 2369-2388.
- Lin, P., Huang, B., Li, Q. and Wang, R. (2014), "Hazard and seismic reinforcement analysis for typical large dams following the Wenchuan earthquake", *Eng. Geol.*, **194**, 86-97.
- Liu, Y., Zhong, D., Cui, B., Zhong, G. and Wei, Y. (2015), "Study on real-time construction quality monitoring of storehouse surfaces for RCC dams", *Automat. Constr.*, **49**, 100-112.
- Luhr, D.R. (2000), *Engineering and Design Roller-Compacted Concrete*, USACE., Washington.
- Monteiro, G. and Barros, R.C. (2008), "Seismic analysis of a roller compacted concrete gravity dam in Portugal", *World Conference of the Earthquake Engineering*.
- Noorzaei, J., Bayagoob, K.H., Thanoon, W.A. and Jaafar, M.S. (2006), "Thermal and stress analysis of Kinta RCC dam", *Eng. Struct.*, **28**, 1795-1802.
- Raphael, J.M. (1984), "Tensile strength of concrete", *J. Proc.*, **81**, 158-165.
- U.S. Army Corps of Engineers (2016), "Earthquake design and evaluation for civil works projects", *USACE*, **2**, 1110-1806.
- U.S. Army Corps of Engineers (1995), "Gravity dam design", *USACE Eng. Man.*, **88**.
- Wang, G., Wang, Y., lu, W., Zhou, W. and Zhou, C. (2015), "Integrated duration effects on seismic performance of concrete gravity dams using linear and nonlinear evaluation methods", *Soil Dyn. Earthq. Eng.*, **79**, 223-236.
- Wilson, E.L. and Khalvati, M. (1983), "Finite elements for the dynamic analysis of fluid-solid systems", *Int. J. Numer. Meth. Eng.*, **19**, 1657-1668.
- Yazdani, Y. and Alembagheri, M. (2017), "Nonlinear seismic response of a gravity dam under near-fault ground motions and equivalent pulses", *Soil Dyn. Earthq. Eng.*, **92**, 621-632.
- Yilmazturk, S.M., Arici, Y. and Binici, B. (2015), "Seismic assessment of a monolithic RCC gravity dam including three dimensional dam-foundation-reservoir interaction", *Eng. Struct.*, **100**, 137-148.
- Zhang, S. and Wang, G. (2013), "Effects of near-fault and far-fault ground motions on nonlinear", *Soil Dyn. Earthq. Eng.*, **53**, 217-229.
- Zhang, X.F., Li, S.Y., Chen, Y.L. and Chai, J.R. (2009), "The development and verification of relocating mesh method for the computation of temperature field of RCC dam", *Adv. Eng. Softw.*, **40**, 1119-1123.

AT

Notations

- ρ : density of water
- B_f : strain-displacement matrix of the fluid element
- ρ_r : reservoir bottom material
- S_f : stiffness matrix of the free surface of the fluid system
- C : wave speeds for the material on the reservoir bottom
- \dot{U}_f : nodal velocity vector
- C_r : wave speeds for the material on the reservoir side
- M_f : mass matrix of the fluid system
- P : stress
- H : matrix consisting of interpolation functions of the fluid element
- C_{11} : bulk modulus
- U_n : normal component of the interface displacement
- ε_v : volumetric strains of the fluid
- M_c : mass for the coupled system

- U_f : nodal displacement vector
- C_c : damping for the coupled system
- K_f : stiffness matrix of the fluid system
- K_c : stiffness matrices for the coupled system
- C_f : elasticity matrix consisting of diagonal terms
- α : constants which depend on cohesion
- k : constants which depend angle of internal friction
- S_{ij} : the deviatoric stresses